

Induced Infrared Absorption due to Bound Charge in the Silver Halides*

RICHARD C. BRANDT†† AND FREDERICK C. BROWN

Department of Physics and Materials Research Laboratory, University of Illinois, Urbana, Illinois

(Received 30 December 1968)

Induced infrared absorption due to polarons generated by band-to-band light has been studied in AgBr and AgCl at low temperatures. Strong narrow zero-phonon lines with sideband structure are observed. The positions of the sharp far-infrared absorption lines indicate that exciton or bound polaron states of large radius are involved. The results are compared with a nonadiabatic theory for bound polarons. An unusual and extremely slow *logarithmic* decay of the induced absorption is observed, together with a logarithmic dependence of the induced absorption on the generating intensity. A model consisting of separated electron and hole polaron pairs, as well as alternative models, is discussed.

I. INTRODUCTION

FOR the last several decades, extensive investigations have been made on color centers in the alkali halides. By way of contrast, no convincing observations of visible color centers have been reported for the silver halides, which are similar to the alkali halides in many ways. Stasiw¹ has interpreted absorption which appears with the addition of chalcogen impurities as color-centerlike absorption, possibly due to *F* centers. However, these results may be due to alteration of the fundamental edge produced by defects. For example, the work of Brothers and Lynch² has indicated that a similar color-center absorption in the thallos halides is really the exciton absorption shifted into the visible region by the presence of an impurity. Although optical measurements have not revealed the existence of color centers in the silver halides, transport experiments do indicate the existence of shallow electron traps which are quite important at low temperature.^{3,4} It has long been suspected that charged trapping centers are of small depth in the silver halides because of the large dielectric polarizability of these materials. The experiments reported here were undertaken to both identify these electron traps and to search for infrared color-center absorption. Measurements were made from 33 to 10 000 cm^{-1} . Concurrent with this work, a paper appeared in the Russian literature⁵ which predicted that *F*-center absorption if present at all in AgBr should appear in the far infrared.

II. METHOD AND APPARATUS

The optical samples were prepared by cutting and polishing single crystals of AgBr and AgCl to thick-

nesses ranging from approximately 6 μ –3 mm. The thin samples (6–40 μ thick) were cut on an American Optical sliding microtome, while the thick samples (0.1–3 mm thick) were cut using a tungsten carbide saw. The thick samples were polished by a combination of mechanical polishing and etching in solutions of 3–5% by weight KCN in water. The thin samples were lightly etched to improve their surfaces. In addition, some of the thick samples were etched and polished until Laue back-reflection x-ray photographs showed negligible surface deformation. They were also annealed near their melting point for 12 h in an inert atmosphere. Since these last two treatments did not have a measurable effect on the induced absorption, samples were normally only polished until they appeared to have a smooth surface when viewed under a red safelight.

The samples were mounted in a Dewar that was a modification of one described by Dutton and Maurer.⁶ A calibrated germanium thermometer and a small mirror were attached to the sample mount. The exciting light entered the cryostat at right angles to the infrared beam and was reflected onto the sample by this small mirror, as shown in Fig. 1. For measurements at frequencies less than 320 cm^{-1} , a removable chamber with sapphire windows was used so that the sample could be immersed in helium gas for heat-exchange purposes. With a He pressure of about 1 Torr in the can, tests

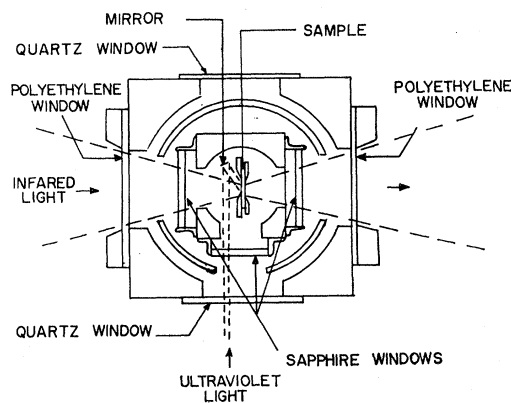


FIG. 1. Horizontal cross section of the tail portion of the helium cryostat showing sample position, cold windows, etc.

* Supported in part by the Advanced Research Projects Agency under Contract No. SD-131 and by U. S. Army Research Office under Contract No. ARO(D)-217.

† Work performed in partial fulfillment of the requirements for the Ph.D. degree at the University of Illinois. A preliminary report is to be found in *Bull. Am. Phys. Soc.* **12**, 316 (1967) and also in *Localized Excitations in Solids*, edited by R. F. Wallis (Plenum Press, Inc., New York, 1968).

†† Present address: Massachusetts Institute Technology Lincoln Laboratory, Lexington, Mass.

¹ M. Stasiw, *Phys. Status Solidi* **8**, 139 (1965).

² A. D. Brothers and D. W. Lynch, *Phys. Rev.* **159**, 687 (1967).

³ R. S. Van Heyningen, *Phys. Rev.* **111**, 462 (1958).

⁴ G. Smith, *Phys. Rev.* **140**, A221 (1965).

⁵ V. M. Buimistrov, *Fiz. Tverd. Tela* **5**, 3264 (1963) [English transl.: *Soviet Phys.—Solid State* **5**, 970 (1963)].

⁶ D. Dutton and R. J. Maurer, *Phys. Rev.* **90**, 126 (1953).

showed that the temperature of the sample ranged from 7.0 to 9.3°K; without the exchange gas the temperature ranged from 23 to 25°K. Polyethylene was used for the outer windows at frequencies less than 200 cm^{-1} , and at higher frequencies CsI windows were employed. The sample Dewar was placed at the focal point of a beam condenser, designed to fit in the sample compartments of Beckman IR-11 and IR-9 double-beam infrared spectrophotometers.⁷ Water-cooled silicon filters placed immediately in front of the sources (a mercury lamp in the IR-11 and a Nernst glower in the IR-9) absorbed all of the visible and ultraviolet light that normally would have been focused on the sample. In addition, the second chopper (the light recombining chopper) of the IR-11 was stopped and held in a beam splitting position to avoid negative light flux effects. The exciting light source was an Osram HBO 200 high-pressure mercury lamp, dispersed with a Bausch and Lomb model 33-86-25 grating monochromator. The intensity of the exciting light was varied by means of neutral density filters.

III. EXPERIMENTAL RESULTS

The steady-state induced infrared optical density was obtained in the following manner. First, the optical density of a sample that had been cooled in the dark was measured over a range of infrared frequencies; second, the sample was illuminated by an intense ultraviolet or near ultraviolet light whose frequency exceeded the indirect band-gap frequency of the sample. While this intense band-to-band light was illuminating the sample, the long-wavelength optical density was remeasured over the same range of infrared frequencies as before. The induced optical density (which we shall often refer to as the induced infrared absorption) is defined as the difference between these two measured infrared optical

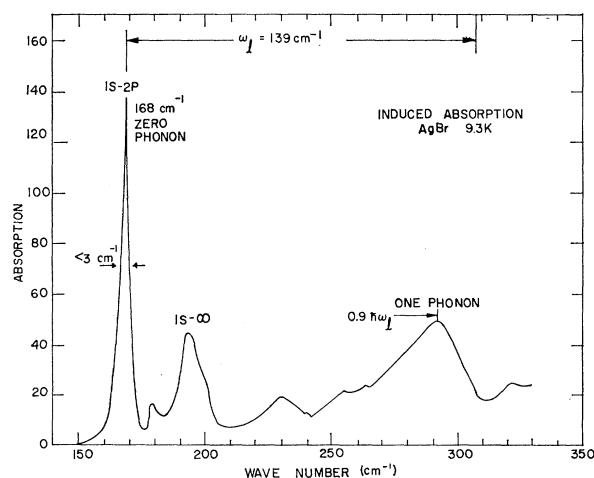


FIG. 2. Induced absorption in AgBr at 9.3°K from 150 to 320 cm^{-1} . The exciting light was in the region of the indirect absorption edge.

⁷ R. C. Brandt, Appl. Opt. 8, 315 (1969).

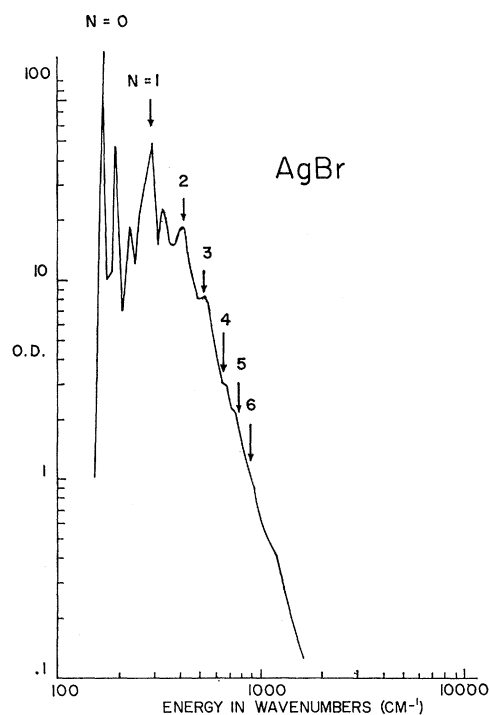


FIG. 3. Composite plot of induced absorption in AgBr from 160 to 1200 cm^{-1} . The values of N denote the number of phonons emitted in the absorption process. Note that both the ordinate and abscissa are logarithmic.

densities. In AgBr this induced infrared optical density or absorption is quite strong and can be measured accurately. Figure 2 shows the region of the most intense induced optical density. The absorption constant for the most intense absorption line at 168 cm^{-1} was as high as 75 reciprocal centimeters in some crystals. Although the absorption constant for the strongest line varied from crystal to crystal, the appearance or structure of the induced absorption was the same. In particular, the ratio of the optical density at 168 cm^{-1} (the "zero-phonon line," see Fig. 2) and that at 292 cm^{-1} (the "one-phonon band") remained constant. In fact, the absorption curve shown in Fig. 2 is composed of data taken from several crystals, normalized so that the absorption at the "one-phonon line" is 50. By varying the crystal thickness, it is possible to obtain data over a wide range of optical density, as shown in Fig. 3. The absorption in AgCl at two different temperatures is shown in Fig. 4. The induced absorption in AgCl was much smaller and correspondingly the data showed more scatter. Because the absorption was so much less in AgCl, reproducible data were not obtained for the so-called "one-phonon" sideband.

The most striking characteristic of the steady-state induced absorption in AgBr is the extreme narrowness of the low-frequency absorption lines as compared to the higher-frequency absorption bands. To determine whether the broad band absorption is associated with the same center as the narrow lines, the temperature

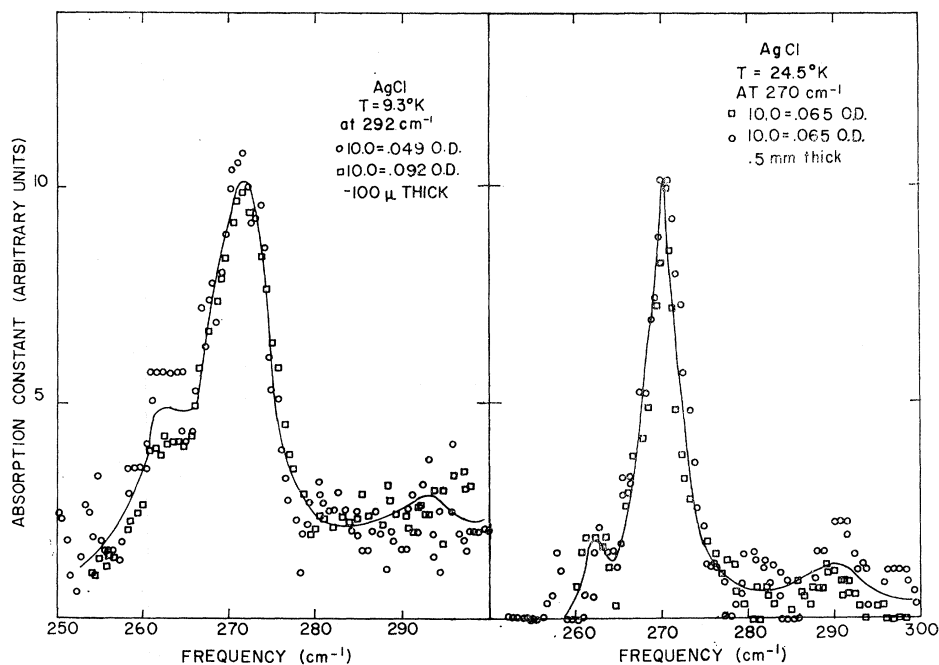


FIG. 4. Induced absorption in AgCl at 9.3 and 24.5°K. The signal-to-noise ratio was much poorer in AgCl than in AgBr.

dependence of the 168-cm^{-1} line and the 292-cm^{-1} band has been measured. The temperature dependence is identical; it is characterized by no change in the induced absorption to 15°K , then there is a *linear* drop in the absorption to about 20% of its initial value at 35°K . Above that temperature the absorption drops more slowly. Data were not taken above 50°K .

The decay of the induced absorption upon turning off the exciting light was measured for several crystals at 7°K . Results are shown in Fig. 5. Note that in this figure the time is plotted logarithmically while the absorption constant is plotted linearly. In normal exponential decay the number present (or the absorption) is plotted logarithmically while the time is linear. Here the absorption depends logarithmically on the time. This peculiar form of decay does not change with increased temperature, although the amplitude of the absorption and the slope of the curves change somewhat, as shown in Fig. 6. The dependence of the induced absorption on the intensity of the ultraviolet exciting light is also logarithmic, as is shown in Fig. 7. The scatter in the data points is not fully understood, but may be associated with the wire-grid neutral density filters used.

Several additional experiments have been tried with negative results. First, we have looked for infrared luminescence associated with the induced infrared absorption. Over the region examined, $40\text{--}800\text{ cm}^{-1}$, the signal-to-noise ratio was such that luminescence would have been detectable whose intensity at a given frequency exceeded one-tenth the intensity of a room-temperature blackbody source at that frequency. No luminescence was observed. Second, a search was made for a magnetic moment associated with the induced

infrared absorption.⁸ A sample was inserted into the microwave cavity of an ESR-ENDOR apparatus, which permitted illumination of the samples from the bottom of the cryostat using the same light source employed in the infrared experiments. No resonance was found which depended upon illumination. Third, we tried to observe infrared absorption due to free carriers. Since conductivity and loss experiments on the silver halides at low temperature indicate a lifetime of microseconds, the absorption corresponding to free-carrier absorption should be observable by modulating the exciting light instead of the infrared light. A signal at the exciting-light frequency of 15 Hz was detectable but was so much smaller (by a factor of 1000) than the normal chopped infrared signal that the investigation was not pursued. Finally, an attempt was made to correlate the induced absorption to the amount of alloying of AgCl in AgBr. Induced absorption was seen in all the mixed crystals prepared by Joesten and Brown⁹ and in fact it was very intense in some cases. However, no direct correlation could be made between the amount of AgCl in AgBr at low concentration.

IV. DISCUSSION OF RESULTS

A. Energy Levels of the Bound Polaron

The induced absorption consists of sharp lines at low frequencies which resemble zero-phonon transitions and broad bands at higher frequencies which with their repetitive structure are suggestive of phonon sidebands. The fact that both the low-frequency absorption at

⁸ The authors are grateful to Professor R. Miehler, Dr. D. Daly, and Y. Chew of Purdue University for these tests.

⁹ B. L. Joesten and F. C. Brown, Phys. Rev. **148**, 919 (1966).

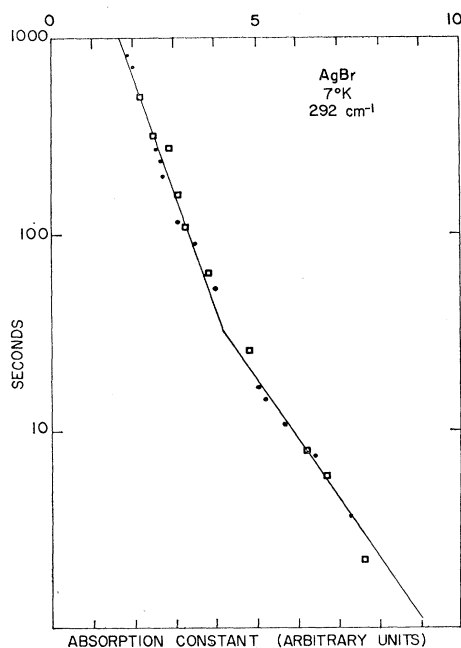


FIG. 5. Time decay of induced absorption in AgBr at 292 cm^{-1} and 7°K . The time in seconds, shown on the ordinate, is the time elapsed after the exciting light has been turned off.

168 cm^{-1} and the broad band absorption which peaks at 292 cm^{-1} in AgBr depend on the temperature identically (the induced optical density keeping its low-temperature value up to 15°K and then decreasing linearly with increasing temperature) convinces us that both absorptions are associated with transitions at the same center in the crystal and that the higher-frequency absorption bands are phonon emission sidebands of the low-frequency absorption. The zero-phonon transitions will be shown to be electronic transitions in a potential field which is probably Coulombic at large distances [actually transitions of polarons since electrons are fairly strongly coupled to longitudinal optical (LO) phonons with coupling constants $\alpha=1.7$ and 2.0 in

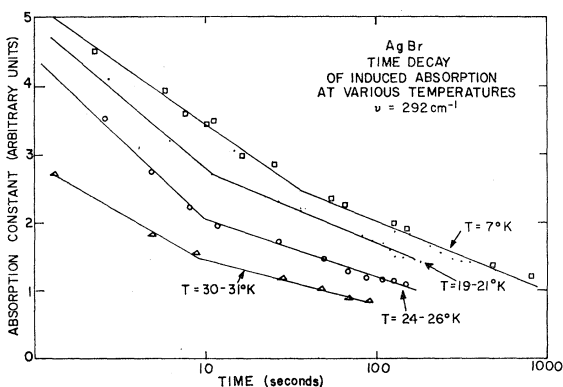


FIG. 6. The time decay of the induced absorption in AgBr at 292 cm^{-1} at various temperatures.

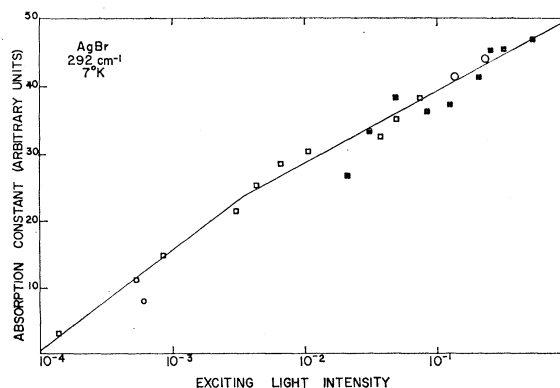


FIG. 7. The induced absorption in AgBr at 292 cm^{-1} versus the intensity of the exciting light. Data from three different runs are included and have been normalized at high intensity.

AgBr and AgCl, respectively¹⁰]. Furthermore, the transitions are most likely electron (polaron) transitions rather than hole transitions since transport experiments on AgBr show that holes are trapped at temperatures up to 120°K , which is well above the range of measurable induced infrared absorption.

The problem of the polaron bound by a Coulomb field has been investigated by Buimistrov and Pekar,¹¹ Platzman,¹² and most recently by Buimistrov.⁵ All three investigations used a variational technique and a Gaussian trial wave function.¹³ For AgBr, the Platzman solution with its three variational parameters gives a lower value for the bound $1s$ state than the Buimistrov-Pekar solution with its one variational parameter. The difference between these two results is about 3%. A better variational wave function for a polaron in a Coulomb field, at least for weak coupling, would be hydrogenlike because in the limit of zero coupling between the electron and the phonons, the exact wave function for the electron is hydrogenlike. We were able to extend the Buimistrov-Pekar approach to permit the use of not only hydrogenlike wave functions but also to allow for arbitrary potentials. It was found that for the simple Coulomb potential and AgBr, the hydrogenlike wave function with only one variational parameter (the radius of the orbit) gives a $1s$ energy which is 4.5% lower than the $1s$ energy using the theory of Platzman.¹²

The basis of the Buimistrov-Pekar approach¹¹ is the separation of the lattice normal coordinates into two

¹⁰ J. W. Hodby, J. A. Borders, F. C. Brown, and S. Foner, *Phys. Rev. Letters* **19**, 952 (1967).

¹¹ V. M. Buimistrov and S. I. Pekar, *Zh. Eksperim. i Teor. Fiz.* **32**, 1193 (1957) [English transl.: *Soviet Phys.—JETP* **5**, 970 (1957)].

¹² P. M. Platzman, *Phys. Rev.* **125**, 1661 (1962).

¹³ Both the Platzman and Buimistrov solutions as printed contain typographical errors. The Buimistrov solution for the $2p$ state contains the multiplicative constant $49/60$; it should be $\frac{2}{3}$. The square-root sign is omitted in the fourth term of the Platzman expression. Actually, Schultz in his unpublished M.I.T. thesis, p. 191-193 (1956), solved the same problem as Platzman did but either did not find or omitted the function that goes into the denominator of the integral appearing in the Platzman expression.

parts, $q_k = q_k' + q_k^0(r)$, where $q_k^0(r)$, the "equilibrium" position of the normal coordinate, depends on the *instantaneous* electron position. The Hamiltonian in terms of the original normal coordinates is

$$\mathcal{H} = -\frac{\hbar^2}{2m}\Delta + \sum_k \frac{1}{2}\hbar\omega_k \left(q_k^2 - \frac{\partial^2}{\partial q_k^2} \right) + \sum_k c_k q_k X_{-k}(r) + V(r), \quad (1)$$

where m is the fixed lattice mass, ω_k is the LO phonon frequency,

$$c_k = -\frac{e(4\pi\hbar\omega_k\epsilon)^{1/2}}{|\mathbf{k}|}, \quad X_k(r) = \begin{pmatrix} 2 \\ - \\ v \end{pmatrix}^{1/2} \sin(\mathbf{k}\cdot\mathbf{r} + \frac{1}{4}\pi), \quad (2)$$

$$c = \frac{1}{n^2} \frac{1}{\epsilon},$$

and $V(r)$ is the potential energy due to the interaction with the positive charge center. The interaction of the LO phonons with the positive charge will be included implicitly by screening the positive charge center with the static rather than the optical dielectric constant. Three different forms for $V(r)$ have been considered, each corresponding to a different distribution of the positive charge. The three different configurations for the positive charge center are: (1) a positive point charge; (2) a uniform positive charge density spread over a spherical volume; (3) a kind of symmetrized V_k center distribution which consists of a negative charge in a spherical volume bounded by $r = ga$ (where g is some fraction) surrounded by a shell of positive charge. In this last case the total charge is adjusted so that the potential for $r > 2ga$ appears to be due to a single positive electronic charge. The three forms for $V(r)$ are then

$$\begin{aligned} V_1(r) &= -e^2/\epsilon r, & V_2(r) &= -e^2 r^2/\epsilon g^3 a^3, & r < ga \\ & & &= -e^2/\epsilon r, & r > ga \\ V_3(r) &= +e^2 r^2/\epsilon g^3 a^3, & r < ga \\ &= e^2/\epsilon r [1 - 2(r^3 - g^3 a^3)/7g^3 a^3], & ga < r < 2ga \\ &= -e^2/\epsilon r, & r > 2ga, \end{aligned} \quad (3)$$

where a is the radius of the first Bohr orbit calculated by

TABLE I. Best available low-temperature values of polaron mass, fixed lattice mass, longitudinal-optical-mode frequency, and dielectric constants for the silver halides.

	Polaron mass ^a	Fixed lattice mass	ω_{LO} ^b	ϵ^c	n^2 ^d
AgBr	(0.33 ± 0.03) m_e	(0.24 ± 0.02) m_e	139 ± 1 cm ⁻¹	10.6 ± 0.1	4.62
AgCl	(0.51 ± 0.04) m_e	(0.35 ± 0.03) m_e	197 ± 1 cm ⁻¹	9.5 ± 0.1	4.04

^a Reference 10.

^b Measured directly at 7°K using a variation of the Berreman technique. D. W. Berreman, Phys. Rev. **130**, 2193 (1963). See also R. Brandt, Appl. Opt. (to be published).

^c R. P. Lowndes, Phys. Letters **21**, 26 (1966).

^d It has been shown that the index of refraction changes less than 1% from room- to liquid-helium temperature [J. A. Borders (private communication)].

using the fixed lattice mass and the static dielectric constant, as in Eq. (4). The zero-point energy of the lattice is omitted and we use units defined as follows:

$$E = 13.6(m/m_e)(1/\epsilon^2) \text{ eV}, \quad a = 0.529\epsilon(m_e/m) \text{ \AA}, \quad (4)$$

$$t = \beta a, \quad s = \delta a, \quad b = 4E/\hbar\omega, \quad b' = E/\hbar\omega.$$

Assuming that the LO phonon frequency is dispersionless, and the $1s$ wave function is of the form $\psi_{1s} = (\beta^3/\pi)^{1/2} e^{-\beta r}$, we obtain the following results:

$$\frac{H_{1s}(t)}{E} = t^2 - 2t - \frac{15}{48}\epsilon c - \frac{4\epsilon c t}{\pi} \times \int_0^\infty \frac{dx [1 - (1+x^2)^{-4}]^2}{b'^2 x^2 + 1 - (1+x^2)^{-4}} + \langle V(r) \rangle_{1s}, \quad (5)$$

with

$$\langle V_1(r) \rangle_{1s} = -2t, \quad (5')$$

$$\langle V_2(r) \rangle_{1s} = -\frac{1}{2} \left\{ \int_0^{2\theta t} x^2 e^{-x} dx \frac{-x^3}{2t^2 g^3} + \int_{2\theta t}^\infty x^2 e^{-x} dx \frac{-4t}{x} \right\}, \quad (5'')$$

$$\langle V_3(r) \rangle_{1s} = \frac{1}{2} \left\{ \int_0^{2\theta t} x^2 e^{-x} dx \frac{x^3}{2t^2 g^3} + \int_{2\theta t}^{4\theta t} x^2 e^{-x} dx \left[\frac{4t}{x} - \frac{8t}{7x} \left(\frac{x^3}{8t^3 g^3} - 1 \right) \right] + \int_{4\theta t}^\infty x^2 e^{-x} dx \frac{-4t}{x} \right\}. \quad (5''')$$

For

$$\psi_{2p} = (\delta^5/32\pi)^{1/2} r e^{-\delta r/2} \cos\theta,$$

we obtain

$$\frac{H_{2p}(s)}{E} = \frac{s^2}{4} - \frac{s}{2} \left[\frac{63}{256} \epsilon c \left(8.4 - 20.8 \times \frac{11}{12} + \frac{143}{168} \times 14.4 \right) \right] - \frac{\epsilon c s}{\pi} \int_0^\infty dx \int_{-1}^{+1} \left\{ d\mu \left[1 - \frac{(1+x^2(1-6\mu^2))^2}{(1+x^2)^8} \right]^2 / \left(b'x^2 s^2 + 1 - \frac{(1+x^2(1-6\mu^2))^2}{(1+x^2)^8} \right) \right\} + \langle V(r) \rangle_{2p}, \quad (6)$$

with

$$\langle V_1(r) \rangle_{2p} = -\frac{1}{2}s, \quad (6')$$

$$\langle V_2(r) \rangle_{2p} = \frac{1}{24} \left\{ \int_0^{gs} x^4 e^{-x} dx \frac{-2x^3}{s^2 g^3} + \int_{gs}^\infty x^4 e^{-x} dx \frac{-2s}{x} \right\}, \quad (6'')$$

$$\langle V_3(r) \rangle_{2p} = \frac{1}{24} \left\{ \int_0^{gs} x^4 e^{-x} dx \frac{2x^3}{s^2 g^3} + \int_{2gs}^{\infty} x^4 e^{-x} dx \frac{-2s}{x} \right. \\ \left. + \int_{gs}^{2gs} x^4 e^{-x} dx \left[\frac{2s}{x} - \frac{4s}{7x} \left(\frac{x^3}{s^3 g^3} - 1 \right) \right] \right\}. \quad (6''')$$

All the constants appearing in the above expressions, except for the fixed lattice mass, have been measured directly. The fixed lattice mass was obtained from the data of Hobdy *et al.*¹⁰ by using a formula of Langreth,¹⁴ which closely approximates the Feynman¹⁵ polaron mass to fixed-lattice-mass relation. These constants are given in Table I. To compute the position of the continuum or polaron self-energy, the expression of Hohler and Müllensiefen¹⁶ is used.¹⁷

The theoretical values for the $1s-2p$ and the $1s$ -continuum transitions are obtained by numerically minimizing the expressions for the $1s$ and $2p$ levels for the three potentials. The factor g appearing in the expressions was arbitrarily taken to be equal to $\frac{1}{10}$ ($g=0.1$ in the case of V_3 , is roughly equivalent to setting the radius of the positive charge density ga slightly greater than the nearest-neighbor distance). A 96-point Laguerre Gaussian quadrature was used to compute the integrals. The results are given in Table II, part A.¹⁸ For all three

¹⁴ D. C. Langreth, Phys. Rev. **159**, 717 (1967).

¹⁵ T. D. Schultz, Phys. Rev. **116**, 526 (1960).

¹⁶ G. Hohler and A. M. Müllensiefen, Z. Physik **157**, 159 (1959).

¹⁷ Initially, in an attempt for self-consistency, we used the formulation of Buimistrov and Pekar {V. M. Buimistrov and S. I. Pekar, Zh. Eksperim. i Teor. Fiz. **33**, 1271 (1957) [English transl.: Soviet Phys.—JETP **6**, 977 (1957)]} for the self-energy using a translationally invariant wave function. We avoided their approximations by numerically integrating their first expression for the self-energy rather than using the approximate expressions they derived in order to get an analytical expression. This formulation gave better values for the self-energy than the Feynman expression [R. P. Feynman, Phys. Rev. **97**, 660 (1955)] for values of α less than 6. For instance, at $\alpha=3$, the Buimistrov-Pekar self-energy is 3.211 while the Feynman value is 3.133. However, as α went to zero (to investigate this the self-energy was computed for $\alpha=1, 0.5, 0.2$, and 0.1), the Buimistrov-Pekar self-energy exhibited two minima, one equal to $-\alpha$, the other having a value slightly lower than the perturbation theory expression $-(\alpha+0.01592\alpha^2)$; that is, the Buimistrov-Pekar self-energy expression is too low (as α goes to zero) as we computed it, and therefore either our computer programs or the expression of Buimistrov and Pekar is incorrect. Until the error is found, we will use the perturbation theory expression at small α .

¹⁸ The $2p$ state appears not to be bound because of our probably incorrect treatment of the effects of the lattice polarization for the reduced-mass case. To see how this may occur we will examine the effects of the lattice polarization in lowest order. First, it lowers the energy of the electron through the electron-phonon interaction; this contribution, called the self-energy, is in lowest order proportional to square root of the fixed lattice mass of the electron. Second, it screens the Coulomb field so that the Coulomb contribution to the energy is reduced by the static dielectric constant. In this lowest order we may then write for the energy of level n

$$E_n = -K(m)^{1/2} - (m/m_e) Ry/n^2 e^2,$$

where by m we mean the fixed lattice mass of the free polaron. Consider now the reduced-mass (m_r) case. Should the energy be

$$E_n^a = -K(m)^{1/2} - (m_r/m_e) Ry/n^2 e^2$$

or

$$E_n^b = -K(m_r)^{1/2} - (m_r/m_e) Ry/n^2 e^2?$$

We do not know; however, the first expression guarantees that the

TABLE II. Comparison of theoretical and experimental transition energies (in cm^{-1}) for the bound polaron in the silver halides.

	AgBr			AgCl		
	m/m_e	$1s-2p$	$1s-\infty$	m/m_e	$1s-2p$	$1s-\infty$
Experiment	0.24	168	192±2	0.35	272	292±3
A. Unadjusted results						
Theory						
V_1	0.24	250	300	0.35	460	560
V_2	0.24	230	290	0.35	400	480
V_3	0.24	190	260	0.35	380	450
B. Reduced-mass results						
Theory	m_r/m_e					
V_1	0.176	168	170	0.22	272	245 ¹⁸
V_2	0.184	168	180	0.254	272	270 ¹⁸
V_3	0.215	168	200	0.266	272	300

potentials the theoretically predicted transitions are larger than the experimental values. (For electrons trapped on impurities in semiconductors the opposite is usually true; the $1s$ state being more tightly bound than predicted by theory.) Since this is a variational calculation, any improvements on the Coulomb ground-state wave function will make the agreement worse.

Better agreement between the theoretical predictions and the experimental data can be obtained by (1) further modification of the potential possibly by increasing the fraction g somewhat, or (2) by replacing the fixed lattice mass m appearing in the Hamiltonian by a slightly smaller reduced mass m_r . Let us consider this second possibility. Results are given in Table II, part B, for values of m_r/m_e chosen so that the theoretical prediction for the $1s-2p$ transition fits the observed position of the zero-phonon line. The third potential V_3 gives the best fit in the sense that the $1s$ to ∞ energy is larger than $1s$ to $2p$ by a reasonable amount. The use of a markedly reduced mass (substantially smaller than the mass obtained by Hobdy *et al.* and well outside the cyclotron resonance experimental error) would seem to require that the positive charge center or some part of it possesses a significant portion of the over-all kinetic energy of the polaron and positive charge center complex. This would be the case if we are dealing with a polaron exciton and the mass of the hole is the same order of magnitude as the mass of the electron. By polaron exciton we mean an exciton where the interaction of hole and electron with the lattice has been included in the calculation of energy levels. This model and alternatives are further discussed in Secs. IV B and IV D.

transition E_{1s-2p}^a is less than $E_{1s-\infty}^a$, since $E_{1s-\infty}^a - E_{1s-2p}^a = (m_r/m_e) Ry/4e^2$. Using the second expression for the energy we find that

$$E_{1s-\infty}^b - E_{1s-2p}^b = (m_r/m_e) Ry/4e^2 - [K(m)^{1/2} - K(m_r)^{1/2}].$$

This expression can either be positive or negative. Since we used the same variational expression (5) and (6) in the reduced-mass case, just substituting the reduced mass wherever a mass occurred, our results will have characteristics similar to those obtained with E_n^b above; that is, the $2p$ state may not be bound.

B. Ultraviolet Absorption and the Bound Polaron

If the bound polaron absorption in the infrared is due to either a free or bound polaron exciton, one would expect there might be some similarities between the induced infrared absorption and the detailed ultraviolet absorption associated with the polaron exciton. Under certain conditions (small radii) the ultraviolet absorption associated with the exciton would have energy levels dependent upon the optical constant n^2 and rigid lattice mass m .¹⁹ For larger radii the lattice polarizability is important and the static dielectric constant and polaron mass are more appropriate as explained in the theory of Haken.²⁰ Present experiments on the indirect absorption edge of AgBr reveal structural details in the absorption whose energy separations are remarkably close to those observed in the induced infrared absorption. These results will be discussed below since they indicate that the important eigenstates for estimating the optical spectra are those of the electron-lattice system.

Strong evidence for the existence of a polaron exciton in AgBr can be found in the recent work of Ascarelli²¹ on piezo modulation of the indirect absorption edge. His exciton binding energies are actually somewhat smaller than the induced infrared absorption energies reported above. This indicates that the induced infrared absorption of the present work is not due to excitons but to a bound electron polaron, perhaps with a somewhat diffuse positive charge center. However, it may be that a detailed comparison of these two kinds of experimental results is not warranted.

Figure 8 shows a high-resolution scan of the indirect edge of AgBr at 4.7°K similar to that previously published.²² A number of reproducible structural details are observable. The well-defined threshold corresponding to the emission of a 65-cm⁻¹ zone boundary phonon, as required for conservation of crystal momentum, occurs at 2.691 eV. Indirect absorption with the emission of a somewhat higher energy phonon (approximately 95 cm⁻¹) sets in beginning at 2.695 eV. Transitions to the higher exciton states and the continuum are not clearly seen in the indirect absorption edge but they probably occur somewhere in the range 2.705–2.715 eV, depending upon exciton binding energy. The broad band labeled $N=1$ peaks at about $0.9\hbar\omega_l$ above the first threshold. The one-phonon sideband in the induced infrared absorption shown in Fig. 2 also peaks at $0.9\hbar\omega_{LO}$. It is probably coincidental that the one-phonon sidebands in the two cases peak at approximately the same fraction of $\hbar\omega_{LO}$ since optical absorption at the indirect exciton threshold is thought to produce $1s$ final

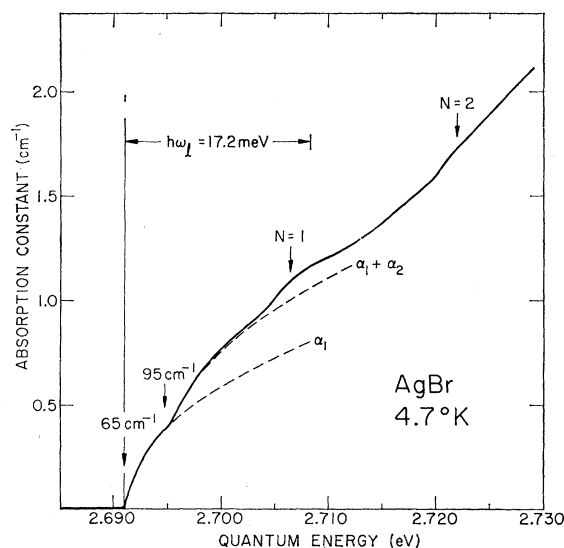


FIG. 8. High-resolution scan of the indirect optical edge of pure AgBr at 4.7°K.

polaron states while the induced infrared absorption results in $2p$ -like final polaron states. However, it is not inconceivable that the phonon sidebands in the two cases are due to similar physical phenomena.

Along somewhat different lines Kanzaki and co-workers²³ have reported mirrorlike absorption and emission bands for AgBr containing iodide. The periodicity of the phonon structure observed in emission (16.5 meV) is found to be near the LO phonon frequency (17.2 meV), whereas the separation of phonon peaks in absorption is considerably less (12.7 meV). An electron-hole binding energy of 19 meV is also reported for excitons in the vicinity of iodine.

Toyozawa and Hermanson²⁴ have recently given theoretical evidence for an exciton plus bound phonon state which is shifted in energy so as to lie below the exciton plus one-phonon continuum of states. (See note added in proof.) Experimental evidence²⁵ for such states has been given for thallos halides, which are similar to the silver halides in several ways. These negative energy shifts occur when one has polaritonlike dispersion curves or "pinning" effects as first observed for polarons in interband magnetoabsorption.²⁶ Pinning effects have been observed for plasmon-phonon interactions²⁷ and for photon-photon interactions.²⁸ The exciton-phonon calculations referred to above²⁴ have so far been carried out

²³ H. Kanzaki, S. Sakuragi, and S. Ozawa, J. Phys. Soc. Japan **24**, 652 (1968); H. Kanzaki and S. Sakuragi, *ibid.* **24**, 1184 (1968).

²⁴ Y. Toyozawa and J. Hermanson, Phys. Rev. Letters **21**, 1637 (1968).

²⁵ R. Z. Bachrach and F. C. Brown, Phys. Rev. Letters **21**, 685 (1968).

²⁶ E. J. Johnson and D. M. Larsen, Phys. Rev. Letters **16**, 655 (1966).

²⁷ A. Mooradian and A. L. McWhorter, Phys. Rev. Letters **19**, 849 (1967).

²⁸ C. H. Henry and J. J. Hopfield, Phys. Rev. Letters **15**, 964 (1965).

¹⁹ R. J. Elliott, Phys. Rev. **108**, 1384 (1957).

²⁰ H. Haken, J. Phys. Chem. Solids **8**, 166 (1959).

²¹ G. Ascarelli, Phys. Rev. Letters **20**, 44 (1968); also Phys. Rev. (to be published).

²² F. C. Brown, T. Masumi, and H. H. Tippins, J. Phys. Chem. Solids **22**, 101 (1961); B. L. Joesten and F. C. Brown, Phys. Rev. **148**, 919 (1966).

only for the one-phonon case. If the multiphonon exciton theory turns out to be analogous to the theory for polaron cyclotron resonance,²⁹ only the first phonon peak would be shifted below $\hbar\omega_l$. The other sidebands would be separated by a more nearly $\hbar\omega_l$ assuming no LO dispersion. This is not in agreement with the induced infrared absorption (Fig. 3) where the periodicity appears to be about 15.4 meV, the same as the separation between the zero- and one-phonon bands. It may be, however, that the $N=1$ band, seen in the ultraviolet absorption just below $\hbar\omega_l$ (Fig. 8), is due to the formation of an exciton-bound LO phonon. States of this type were not properly taken into account in the Buimistrov-Pekar approach discussed in Sec. IV A.

The phonon sidebands can be analyzed phenomenologically by assuming that the first phonon sideband has the same shape as the phonon spectral emission function and that the phonons are emitted randomly. In this case, the two-phonon sideband is a convolution of the first sideband; the three-phonon sideband is a convolution of the first and second sideband, and so on for higher orders. When the data are fitted in this way, it is found that: (1) not all phonon information is contained in the one-phonon sideband since there is emission associated with the 1s-continuum transition as well as the 1s-2p transition; (2) Huang-Rhys factor³⁰ which gives the best fit is 1.5 ± 0.2 . The broad bands observed also indicate that phonons of many different wave vectors are emitted. The diffuse bound polaron states would be expected to couple only to long wavelength or equivalently small wave-vector phonons. As result we think that the phonon sidebands are probably primarily due to the lattice response to changes of the charge distribution in the vicinity of the positive charge center. Since the phonon sidebands are relatively broad this requires that the positive charge center be relatively well localized, probably on some sort of defect in the crystal.

C. Kinetics for Generation and Decay of Bound Polaron States

In Fig. 5 we plotted the intensity of the induced absorption after the exciting light is turned off. Similar data are shown in Fig. 6, except that results are also given for higher temperatures. The similarity of the decay curves at different temperatures shows that ordinary thermal generation is not of primary importance in the decay of the bound polaron states. With this in mind let us examine the low-temperature (7°K) data shown in Fig. 5. These data can be fitted approximately by the following equation:

$$I = 10\,000e^{-13.7x} + e^{6.4x}/17, \quad (7)$$

where t is the time in seconds and x is the fraction of the steady-state absorption left at time t . For simplicity, and to permit an analytic solution for x , let us retain only the first part of the equation (the second part is only important for short times and x near 1.0). The quantity x and its derivative with respect to time are then given by

$$x = (\ln 10\,000 - \ln t)/13.7 \quad (8)$$

and

$$dx/dt = -1/13.7t = -e^{13.7x}/137\,000, \quad (9)$$

where the range of validity of these expressions are for the time t between 10 and 1000 sec. Equation (8) shows that the fraction x decays logarithmically instead of exponentially, and so the decay is not monomolecular but probably involves at least two bodies at different locations in the crystal. Assuming radiative decay, Eq. (9) indicates that the emission would decrease as $1/t$ after the exciting light is turned off.

Finally, let us consider what would happen if we illuminated the crystal with various constant generating intensities in order to measure the steady induced absorption as a function of the intensity of the exciting light. The steady-state fractional absorption should obey a relation which can be obtained by setting dx/dt equal to zero in Eq. (9) and adding a constant generation rate proportional to light intensity I . The result is as follows:

$$dx/dt = -e^{13.7x}/137\,000 + \alpha I = 0 \quad (10)$$

or

$$I = e^{13.7x}/\beta, \quad (11)$$

where α and β are constants. An experiment to test this last result was performed and the results are shown in Fig. 7. The data for the low-intensity portion of the curve in Fig. 7 are in agreement with the following equation:

$$R = e^{7.8x'}/11\,200, \quad (12)$$

where R is the ratio of the intensity of the exciting light that generates the fractional absorption x' to the most intense exciting light I_0 . The units are given in Fig. 7. This is the solution predicted by Eq. (11), except for arbitrary constants related to the method of plotting. Thus, the decay and generation kinetics are consistent with each other.

D. Possible Models for the Infrared Centers

The unusual logarithmic decay of the induced absorption indicates that the exponential tails of overlapping wave functions may be involved. This would be the case for a triplet-exciton model and also for pairs of widely separated electrons and holes.³¹ Let us briefly discuss the former and then turn to the separated electron-hole pair model.

Although the reduced mass arguments given toward the end of Sec. IV C argue for excitons, the lifetime of

²⁹ D. H. Dickey, E. J. Johnson, and D. M. Larsen, Phys. Rev. Letters **18**, 599 (1967).

³⁰ K. Huang and A. Rhys, Proc. Roy. Soc. (London) **204A**, 406 (1950).

³¹ D. G. Thomas, J. J. Hopfield, and W. M. Augustyniak, Phys. Rev. **140**, A202 (1965).

singlet-exciton states is usually orders of magnitude shorter than the observed decay of the induced absorption. A triplet exciton, however, might have the long lifetime and could decay by overlap with another such state of opposite spin. This can be shown to lead to the observed decay and generation kinetics, either by overlap of electron wave functions or by the overlap of electron and hole wave functions on different sites. The triplet exciton could be formed in either of two ways: (1) either directly by band-gap light after which the exciton may or may not be localized by an impurity; (2) or indirectly by band-gap light producing free electrons and holes. The holes then rapidly trap out at neutral defects or impurities so that electrons with parallel spin can become trapped in the Coulomb field of the trapped hole.

The identity of the hole traps is unknown. Relatively deep (0.4 eV) hole traps in AgBr³² have been found to have very large cross sections and to be relatively few in number (10^{10} – 10^{11} cm⁻³). On the other hand, iodine is known to be a hole trap and a recombination center, at least in AgCl.³³ The samples used in the present experiments were analyzed both by emission and by mass-spectrographic analysis. The emission results rule out heavy metal impurity contents greater than about 0.03 parts per million³⁴; however, the mass analysis shows the presence of iodine in the range of parts per million. Moreover, the Fairchild samples of AgBr were found to contain about three times as much iodine as the Kodak and this is about the ratio of the maximum absorption which could be induced in the two cases.

Preliminary luminescence studies on the AgBr samples also indicate that iodine may be involved. In the Fairchild samples practically all the observed luminescence appears in the iodine band, whereas in the Kodak crystal the observed luminescence is divided between the iodine and another unknown deeper impurity. On the other hand, the luminescence studies illustrate the complexity of the issue, for one could argue that less induced infrared absorption is seen in the Kodak samples because recombination through the unknown deeper impurity is strongly competitive with the process that gives the induced infrared absorption. The luminescence studies, especially lifetime measurements, are continuing.

The second model that of separated electron-hole pairs has been discussed by Thomas, Hopfield, and Augustyniak.³¹ In this case electrons and holes generated by band-to-band illumination trap at separate points in the crystal. Again luminescent decay is via the overlap of wave functions, and analysis shows that for certain parameters and long times, the luminescent intensity is

approximately inversely proportional to time. This is as observed in GaP and CdS³¹ and is also consistent with the decay of induced infrared absorption in AgBr [refer to Eq. (9)]. When the pair luminescence of the II-VI compounds is observed with high resolution, structure is observed which is associated with different pair distances. So far no such structure has been observed for luminescence in the silver halides. Various factors might rule out a high-resolution pair spectrum. The individual components of this spectrum would be very closely spaced because of the high dielectric polarizability. They might not be readily observable either because of linewidth or resolution problems.

Although the pair model may be correct, it seems unlikely that the required densities of charged centers (electron traps) exist before illumination within the volume of the AgBr crystals studied. As mentioned in the Introduction, shallow electron traps do exist. In AgCl these have a depth of about 0.03 eV and densities of 10^{15} cm⁻³.³⁵ Similar low-temperature electron traps are found in AgBr but it is difficult to believe that they are charged. The Hall mobility of photoelectrons was observed in the Kodak AgBr samples and found to be in excess of 10^5 cm²/V sec below 10°K. This is not unreasonably large in view of the freeze-out of optical modes at low temperature but it rules out long-range Coulomb scattering from centers whose density is very much higher than about 10^{13} cm⁻³. Smakula's equation can be used to estimate a lower limit of about 10^{15} cm⁻³ induced infrared centers under high generation rate.

Because of the above difficulties as well as the lack of a pair spectrum in emission, it is reasonable to speculate on the photogeneration of defects. If, for example, the trapped hole defect were to become neutral, the Coulomb term responsible for the pair spectrum³¹ would be absent. A model satisfying this requirement would be as follows. Imagine that after electron-hole generation the hole becomes trapped (perhaps at a neutral defect such as a substitutional I⁻ ion) after which the center becomes stabilized by formation of an interstitial silver ion. In the silver halides, even at low temperature, interstitial ions would tend to diffuse away. This would leave the hole at a complex (iodine plus positive ion vacancy) which is neutral over all. The electron could then conceivably be trapped in the Coulomb field of the interstitial silver ions generated in this way. In this case the trapped electron states would be outside the silver-ion core and some correction to hydrogenlike levels would be involved. Still other models and mechanisms can be imagined, for example, the generation of positively charged defects at the surface or within the volume of the crystal. Actually, one of the simplest models would be that transitions from ground to excited states of polarons trapped at previously existing neutral defects are involved. Optical transitions to existed

³² R. K. Ahrenkiel and R. S. Van Heyningen, *Phys. Rev.* **144**, 576 (1966).

³³ F. Moser, R. K. Ahrenkiel, and S. Lyu, *Phys. Rev.* **161**, 897 (1967).

³⁴ F. Moser, D. C. Burnham, and H. H. Tippins, *J. Appl. Phys.* **32**, 48 (1961).

³⁵ F. C. Brown and K. Kobayashi, *J. Phys. Chem. Solids* **8**, 300 (1959).

states of the free polaron have recently been investigated theoretically.³⁶ However, it is not yet clear that the results of this work can be applied to the trapped or localized polaron in AgBr.

V. CONCLUSIONS

The most important result of the present work is the observation of far-infrared *electronic* absorption bands not far from the reststrahlen in ionic crystals such as the silver halides. This is in contrast to the alkali halides, where the *F* center or other types of color centers give rise to absorption in the visible and ultraviolet regions of the spectrum. Because the observed energies in the silver halides are so small (168 cm^{-1}), large orbit states are involved as required by the uncertainty principle. A long-range Coulomb interaction between electron and positive charge center is almost certainly involved. The observations confirm the prediction of Buimistrov⁵ that the electronic absorption in the silver halides should occur in the far infrared. Furthermore, by introducing a reduced mass, fairly good agreement between the observed and predicted energy levels can be obtained. In addition, a phonon sideband spectrum rich in detail is observed. Finally, the logarithmic dependence of the induced absorption on the intensity of the exciting light

³⁶ J. Devreese and R. Evrard, Phys. Letters **11**, 278 (1964); R. Evrard, *ibid.* **14**, 295 (1965); E. Kartheuser, R. Evrard, and J. Devreese, Phys. Rev. Letters **22**, 94 (1969).

and its decay properties shows that the decay of these excitations is not monomolecular but involves the overlap of at least two wave functions. Different models for the induced infrared centers are discussed, including long-lived excitons and separated electron-hole pairs. Future developments should permit a choice between these alternatives.

Note added in proof. A shift in the one-phonon sideband below $\hbar\omega_l$ can also be produced by a combination of phonon dispersion and anharmonicity as recently shown by J. Devreese, R. Evrard, and E. Karthenser (to be published). This result, however, requires substantially more dispersion and damping than actually observed for these materials.

ACKNOWLEDGMENTS

We appreciate helpful discussions with Professor Y. Toyozawa, Professor Miles Klein, Dr. S. J. Miyake, Dr. D. M. Larsen, and R. Bachrach. We would like to thank Dr. J. Hodby and Dr. J. Borders for providing us promptly with their experimental results so that they could be used in the calculations. We would also like to thank V. Mossoti and J. Phillips for mass spectrographic analysis. Finally, we are greatly indebted to F. Moser and W. West of the Eastman Kodak Research Laboratories and to J. Luvall of the Fairchild Space and Defense Research Laboratories for supplying pure single crystals.